European Journal of Neuroscience, Vol. 22, pp. 2475–2480, 2005

Retinal abnormalities in human albinism translate into a reduction of grey matter in the occipital cortex

Elisabeth A. H. von dem Hagen,[1] Gavin C. Houston,[1] Michael B. Hoffmann,[1,2] Glen Jeffery[3] and Antony B. Morland[1]
[1]Department of Psychology Royal Holloway, University of London, Egham, Surrey TW20 0EX, UK
[2]Universitats-Augenklinik, Magdeburg, Germany
[3]Institute of Opthalmology, University College London, UK

Keywords: albinism, foveal hypoplasia, visual cortex, voxel-based morphometry

Abstract

Albinism is a genetic condition associated with abnormalities of the visual system. Defects in melanin production cause underdevelopment of the fovea, reduced retinal cell numbers and abnormal routing of ganglion cell nerve fibres at the optic chiasm. We examined 19 subjects with albinism and 26 control subjects to determine whether retinal abnormalities affect the structure of the visual cortex. Whole-brain, high-resolution anatomical magnetic resonance imaging volumes from each subject were obtained on a 1.5-T scanner and segmented into grey and white matter. A voxel-wise statistical comparison of grey and white matter volumes in the occipital lobes between the two groups was performed using voxel-based morphometry. Our analysis revealed a regionally specific decrease in grey matter volume at the occipital poles in albinism. The location of the decrease in grey matter corresponds to the cortical representation of the central visual field. This reduction is likely to be a direct result of decreased ganglion cell numbers in central retina in albinism.

Introduction

Human albinism is a heterogeneous genetic disorder characterized by an abnormality in melanin synthesis. The resulting hypopigmentation manifests itself phenotypically to varying degrees in affected individuals. Individuals with albinism are commonly observed to have an absence of a fovea, translucency of the iris, nystagmus and a reduction in visual acuity (Kinnear *et al*., 1985). It appears, however, that in all individuals with albinism the retinofugal pathway is systematically misrouted (Kinnear *et al*., 1985).

Without adequate levels of melanin, the retina does not develop properly. The first study of human albinism noted an underdevelopment of the macular region and the absence of a fovea (Elschnig, 1913). It has since been shown in animal models that there is a decrease in rod photoreceptors in the albino ferret (Jeffery *et al*., 1994), and ganglion cell density in central retina of the Siamese (Stone *et al*., 1978) and albino cat (Leventhal & Creel, 1985), as well as the albino primate (Guillery *et al*., 1984) is significantly reduced.

Hypopigmentation also causes abnormalities along the retinofugal pathway. Normally, ganglion cell axons from nasal retina cross at the optic chiasm and project to the contralateral hemisphere, whereas many temporal retina fibres remain uncrossed and project ipsilaterally. In cases of hypopigmentation, in addition to the normal contralateral projection from nasal retina, a large number of fibres from temporal retina that would normally remain uncrossed cross the chiasmatic midline (Lund, 1965; Creel, 1971; Guillery & Kaas, 1973; Creel *et al*., 1974; Guillery *et al*., 1975). Hence, the proportion of overall retinal fibres projecting to the contralateral hemisphere is increased.

Correspondence: Dr A. B. Morland, as above.
E-mail: a.morland@rhul.ac.uk

Received 17 May 2005, revised 9 August 2005, accepted 1 September 2005

doi:10.1111/j.1460-9568.2005.04433.x

While normal visual input from the eyes forms a contiguous retinotopic map of the contralateral visual field in visual cortex, in cases of hypopigmentation the aberrant additional input from temporal retina can result in changes to this map. Studies in Siamese cat and albino ferret showed that thalamo-cortical connections undergo reorganization so that an independent map of the aberrant input forms adjacent to the mapping of the normal input (Hubel & Wiesel, 1971; Akerman *et al*., 2003). Kaas & Guillery (1973) showed no evidence for thalamo-cortical reorganization in the Siamese cats they studied, but instead the aberrant cortical input from temporal retina was suppressed. Finally, a third pattern of cortical organization has been observed in the albino cat (Leventhal & Creel, 1985), the albino primate (Guillery *et al*., 1984) and human albinos (Hoffmann *et al*., 2003) where the maps of nasal and temporal retina can be interdigitated in a 'hemifield dominance column' arrangement.

Structural abnormalities in the optic chiasm have been observed in human albinos by using magentic resonance imaging (MRI) (Schmitz *et al*., 2003). Specifically, the medial–lateral width of the optic nerves, tracts and the chiasm are significantly decreased, presumably because of the reduced number of ganglion cells from the underdeveloped central retina. Previous work indicates that the magnitude of retinal afferents is reflected in the size of primary visual cortex in humans (Andrews *et al*., 1997). It is likely therefore that primary visual cortex will be reduced in individuals with albinism. However, a previous assessment of cortical structure in human albinos reported no abnormalities (Brodsky *et al*., 1993).

Voxel-based morphometry (VBM) is a voxel-by-voxel comparison of grey or white matter volume between groups (Wright *et al*., 1995; Ashburner & Friston, 2000; Good *et al*., 2001). It has proved very successful in finding both large-scale structural differences across the whole brain, such as those resulting from age (Good *et al*., 2001) and disease (Wright *et al*., 1995; Woermann *et al*., 1999), as well as more

localized, smaller-scale structural differences in groups of interest such as musicians (Gaser & Schlaug, 2003) and taxi drivers (Maguire *et al*., 2000). Because VBM provides a sensitive method for evaluating cortical abnormalities between groups of subjects, we have employed it here to examine whether structural changes are present in the visual cortex of humans with albinism.

The technique described above has allowed us to determine whether reductions in the size of the retinofugal pathway, originating from the absence of a fovea, are transferred to the cortical representation. Importantly, we address whether cortical territory assigned to the central visual field, undergoes volumetric reduction in response to ganglion cell reduction or whether cortical volume is conserved.

Methods

Subjects

We studied 19 subjects with albinism and 26 control subjects. The control subjects had no known ophthalmological or neurological disorders, and had best corrected visual acuity of 1.05 ± 0.05 measured using the Freiburg visual acuity test (Bach, 1996). The control group's ages ranged from 19 to 55 years (mean ± SD 31 ± 9 years), with 17 female subjects. The subjects with albinism had ages ranging from 18 to 65 years (mean 36 ± 13 years), with 13 females. As has been previously reported (e.g. Abadi & Pascal, 1991) the subjects with albinism had a broad range of visual acuities (see Table 1). Of the 19 subjects with albinism, ten had tyrosinase-related oculocutaneous albinism (OCA1) with no functional tyrosinase (OCA1a) or some residual tyrosinase activity (OCA1b), seven had oculocutaneous albinism type 2 (OCA2) and one had ocular albinism (see Table 1). The exact classification into subtypes of albinism was unclear in some of the subjects owing to the difficulty in distinguishing between types with similar pigmentation levels such as OCA1b, OCA2 and ocular albinism (OA). In addition, certain types of albinism are associated with unknown genetic mutations and may therefore not fall into any distinct category. However, patients were referred following clinical diagnosis of albinism that established foveal hypoplasia and abnormal lateralization of visual evoked potential (VEP) recordings. All subjects gave their informed written consent and the study was approved by the Royal Holloway Ethics Committee.

TABLE 1. Gender, age and classification of subjects with albinism

Subject	Gender	Age (years)	Classification of albinism	Visual acuity
1A	F	30	OCA2	0.50
2A	M	45	OCA1b	0.21
3A	F	45	OCA2	0.28
4A	M	35	OCA1a	0.04
5A	F	18	OCA2	0.33
6A	F	57	OCA1a	0.28
7A	F	65	OCA1b	0.32
8A	M	29	OA	0.13
9A	F	24	OCA1	0.20
10A	F	27	OCA2	0.42
11A	F	30	OCA1b	0.06
12A	F	30	OCA1b	0.20
13A	M	35	OCA2	0.31
14A	F	32	OCA	0.31
15A	M	47	OCA1b	0.41
16A	F	23	OCA2	0.40
17A	F	31	OCA2	0.50
18A	F	50	OCA1a	0.12
19A	M	18	OCA1a	0.30

Visual acuity was obtained for the preferred eye for viewing with the Freiburg visual acuity test (Bach, 1996).

MRI and data analysis

Subjects underwent a whole-brain T1-weighted MP-RAGE anatomical scan on a Siemens 1.5-T Magnetom system. Volumes were acquired in the sagittal plane (256 slices covering the whole brain, matrix size 256×256, slice thickness 1.0 mm, inplane resolution 0.98×0.98 mm, echo time 4 ms, repetition time 9.7 ms for a total acquisition time of 10 min 36 s).

Anatomical measurements

The dimensions of the optic nerves, optic tracts and optic chiasm were measured in all subjects from an oblique slice through the three-dimensional image volume, chosen such that the optic nerves, tracts and the chiasm were visible in the same plane (as depicted in Fig. 1A). Measurements were performed by hand by an independent observer who was not aware whether the images were from control subjects or subjects with albinism. Significance levels between groups were determined by the Mann–Whitney test, as data were not distributed normally.

VBM analysis

For the statistical analysis, images were converted to Analyse format and analysed in Matlab 6.5 (MathWorks, Natick, MA, USA) using SPM2 (Wellcome Department of Cognitive Neurology, London, UK). Voxel-wise comparison of grey and white matter between the two groups was performed by using VBM using the optimized protocol detailed in Good *et al*. (2001) and summarized below.

Template creation

A customized, anatomical template was created based on 39 subjects (19 albinos, 20 controls). This involved spatially normalizing each anatomical MRI to the ICBM template (Montreal Neurological Institute, Montreal, Canada), which approximates Talairach space (Talairach & Tournoux, 1988). The normalized images were then segmented into grey matter, white matter and cerebrospinal fluid (CSF). A mean image volume of the normalized T1-weighted anatomical scans was created, as well as mean grey matter, white matter and CSF image volumes. These average image volumes were then smoothed with a Gaussian kernel of 8-mm full-width at half-maximum (FWHM). The mean grey matter, white matter and CSF images were created for use as prior probability maps during segmentation in the optimized VBM protocol.

Optimized VBM

A 12-parameter affine transformation was used to match the original T1-weighted anatomical images with the customized T1 template. The registered images were then segmented into grey matter, white matter and CSF images, and non-brain tissue was removed using an automated brain extraction procedure based on morphological dilations and erosions. Non-linear spatial normalization of the segmented images to the segmented customized priors was then performed to account for shape differences between images. However, because the original segmentation was performed on affine-registered images and the customized priors are in stereotactic space, it is preferable to perform

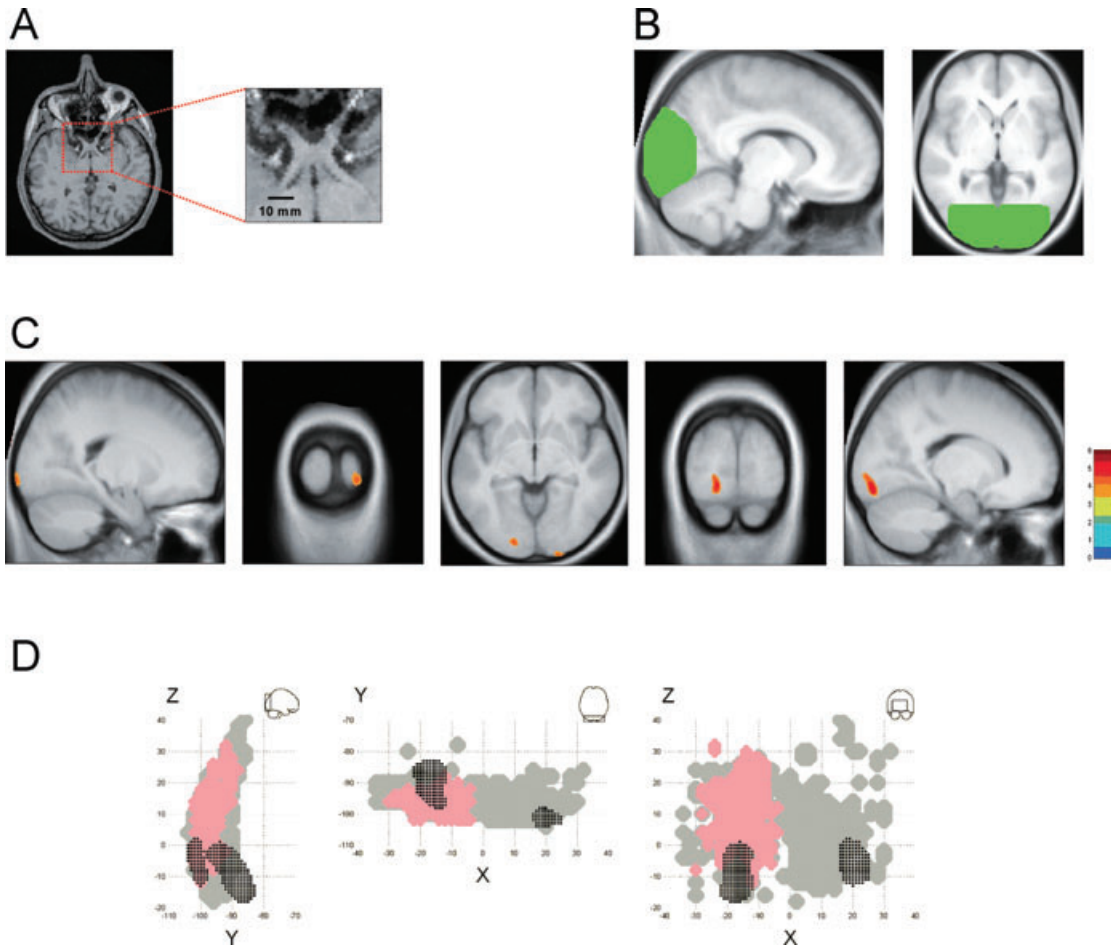

FIG. 1. (A) Oblique slice through the optic chiasm with enlarged volume of interest. (B) Occipital lobe mask for small-volume correction depicted in a sagittal and axial view. (C) Regions of significantly reduced local grey matter volume in albinism overlaid on average T1-weighted anatomical scan sections. Age and total intracranial volume were modelled as nuisance covariates. Significant voxels ($P < 0.05$, small volume corrected) are depicted (from left to right): in a sagittal section at $x = 21$ and in a coronal section at $y = -102$ showing voxels in the right hemisphere; in an axial section at $z = -7$, in a coronal section at $y = -90$ and in a sagittal section at $x = -16$ showing voxels in the left hemisphere. The colour scale bar denotes the t-value. (D) Glass brain views of the areas of activity associated with visual stimulation of the central 2° in four control subjects (grey) and four subjects with albinism (pink). The activity for the subjects with albinism is lateralized to one hemisphere because only one eye was stimulated. The location of reductions in grey matter for subjects with albinism are shown in black. Inset schematics indicate the region of the brain and the orientation of the graphical depictions of the cortical activity and grey matter reduction.

the segmentation on normalized images to optimize tissue classification. The non-linear transformation parameters were therefore applied to the original unwarped anatomical images, which were then segmented and extracted as described above. Segmented images for each subject were examined individually in order to ensure no gross tissue classification errors had occurred. One of the subjects with albinism was removed from further analysis because of a substantial 'zipper' artefact in the images. To ensure further the absence of any bias in image quality between the two groups, grey and white matter peaks were obtained from image intensity histograms of the occipital lobes for each subject. Neither the mean peak intensities nor the mean peak separation between the albino and control groups was significantly different ($P = 0.50$, $P = 0.95$ and $P = 0.18$, respectively, for grey peak, white peak and separation of peaks, by t-test). Thus, there should be no differences between groups based on segmentation difficulties.

Because spatial normalization can cause certain brain regions to shrink or expand, a modulation step was incorporated following the segmentation to take into account any such volume changes. This was done by multiplying the voxel values in the segmented images by the Jacobian determinants from the spatial normalization step. The modulated, segmented images were smoothed using a Gaussian kernel of 10 mm FWHM.

Statistics

Statistical analysis was performed in SPM2 based on the General Linear Model and t-tests were used to determine regionally specific decreases or increases in grey and white matter volume in albinism as compared with controls. Both age and total intracranial volume, calculated as the sum of the modulated grey matter, white matter and CSF images for each subject, were modelled as nuisance covariates to discount the effects of overall head size and grey matter atrophy due to age. Data were first thresholded with an uncorrected P-value < 0.001. Following this, owing to our regional prior hypothesis of changes in grey and white matter volumes in the occipital lobes in albinism, we performed a small volume correction for multiple comparisons, as dictated by Gaussian random field theory (Worsley *et al.*, 1996). The small volume correction was based on an occipital lobe mask (Fig. 1B) and corrected significance levels were set at $P < 0.05$.

TABLE 2. MRI measurements of optic nerve, tract and chiasm widths

	Chiasm width (mm)	Optic nerve width (mm)		Optic tract width (mm)	
		Left	Right	Left	Right
Controls	11.6 ± 1.7	4.5 ± 0.7	4.2 ± 0.6	3.3 ± 0.6	3.4 ± 0.5
Albinos	9.4 ± 1.0	3.6 ± 0.5	3.4 ± 0.3	3.1 ± 0.6	3.2 ± 0.4
P-value	< 0.001	< 0.001	< 0.001	0.07	0.25

Functional imaging procedures

We acquired T2*-weighted images during presentation of expanding ring stimuli in order to establish the cortical representation of visual field in eight of our subjects (four controls, four albinos). Our selection of subjects was limited to four albinos because we could only perform retinotopic mapping in subjects whose nystagmus was less than 1°. Stimuli were presented to one eye only because subjects with albinism had strabismus that would result in different retinal locations being stimulated in the two eyes (see Hoffmann *et al*., 2003). A multislice gradient-echo EPI sequence (TE 54 ms, TR 3 s, 128 × 128 acquisition matrix, field of view 24 cm) was used to acquire data from 12 slices positioned perpendicular to the calcarine sulcus. We acquired 84 volumes with a TR of 3 s, giving a total scan duration of 256 s. During this period three chessboard ring elements undergoing pattern reversal at 6 Hz were presented so that they moved progressively through the central 22° of the visual field. The three ring elements covered 5.7° of eccentricity and resumed their starting position after a 36-s cycle. In total, seven cycles were presented during the scan.

Data were Fourier analysed and correlation to the fundamental frequency of visual stimulation was calculated (Engel *et al*., 1994, 1997). Only voxels with a correlation coefficient greater than 0.24 ($P < 0.05$) were included in further analysis. A phase window was applied to the data to determine the activation resulting from stimulation of the central 2° of visual field – the 'foveal confluence' (Dougherty *et al*., 2003).

Results

There was a significant reduction in the width of the optic nerves and optic chiasm in subjects with albinism (Table 2). These results are in agreement with previously published results (Schmitz *et al*., 2003). Although optic tract width in albinism was also reduced, this reduction was not statistically significant when each tract was considered alone (Table 2), but when averaged the significance increased markedly ($P = 0.03$).

A voxel-by-voxel group comparison of grey matter volume between subjects with albinism and control subjects revealed bilateral areas of significantly decreased grey matter volume in the occipital lobe in albinism. At an uncorrected *P*-value < 0.001, only the occipital poles showed voxels with significant decrease in grey matter volume. No other cortical areas showed significant change (increase or decrease) in grey matter volume. When correction for multiple comparisons was applied across the whole brain, there were no significant regions of change; however, this type of correction is appropriate only in instances where no regional prior hypotheses exist (see Vargha-Khadem *et al*., 1998). Owing to our prior hypothesis regarding visual cortical areas, we applied a correction for multiple comparisons based on an occipital lobe region-of-interest shown in Fig. 1B. Figure 1C depicts the regions of decreased grey matter and their relative *t*-scores (small volume corrected, with age and total intracranial volume modelled as nuisance covariates) overlaid on axial, sagittal and coronal sections through the left and right hemispheres of the mean T1-weighted image based on all subjects' anatomical scans. Significance levels were set at $P < 0.05$ following the small volume correction. The voxel coordinates and statistical test scores are given in Table 3.

To ensure that our results were not in part due to differences in total grey matter volumes between groups, we performed a second analysis. In this analysis global grey matter volume was modelled as a nuisance covariate. The model determines whether the effect observed reflects local or global grey matter differences between groups. The results of this analysis revealed that the clusters identified in the primary analysis remained significant ($P < 0.05$, small volume corrected) and no new significant clusters emerged (see Table 3). We are confident therefore that the reduction in grey matter reported at the occipital poles is local and independent of overall grey matter volume. We also analysed white matter volume in albinism compared with control subjects and no observable change (increase or decrease) in white matter volume was identified.

The extent of the reduction in grey matter is small compared with the area of the occipital lobe that is retinotopically mapped. It appears therefore that the reduced grey matter is specific to cortical tissue that represents only a selective part of the retina. The retinotopic map in

TABLE 3. Voxel coordinates and statistical test scores

Anatomical location	Cluster extent (voxels, mm^3)	*T*-value	*Z*-value	MNI coordinates		
				x	*y*	*z*
Covariates: Age and Total intracranial volume						
Left posterior occipital lobe	1171	5.22	4.53	−16	−88	−13
Right posterior occipital lobe	435	4.24	3.83	21	−102	−6
Covariate: Global grey matter volume						
Left posterior occipital lobe	1077	5.12	4.48	−16	−88	−13
Right posterior occipital lobe	516	4.37	3.94	21	−103	−6

calcarine cortex is well known, with central retina being represented at the occipital pole and more eccentric retinal locations being represented increasingly more anteriorly on the medial aspects of the occipital lobes. The location of the clusters at the occipital pole suggests that the reduction of grey matter is located in the cortical representation of the central retina.

To provide a comparison of the cortical representation of the central visual field with the loci identified in our VBM analysis, we undertook retinotopic mapping experiments to localize the cortical representation of the central 2° in four control and four albino participants. The central 2° was chosen as it has been previously defined as the 'foveal confluence' in a recent functional imaging study (Dougherty *et al*., 2003). Dougherty *et al*. (2003) point out that obtaining topographic mapping of polar angle within the central 2° has not been successfully demonstrated with functional MRI, so visual area boundaries cannot be identified readily in the 'foveal confluence'. In Fig. 1D, the cortical areas responding to stimulation of the central 2° are shown together with the locations of anatomical change in albinism. It is clear from the figure that there is a high degree of overlap between the anatomical abnormalities and the regions of cortex that represent the central 2° of visual field. It should be noted that although the location of activity in the normal and albino subjects is similar, the spatial extent of activity is significantly reduced ($P = 0.02$) for the albinos compared with controls.

Discussion

Here we have shown that there is a specific and local reduction in cortical volume in a region of the albino brain that corresponds to the cortical representation of the central retina. This result was independent of a number of possible comfounding variables. Individual variability in grey matter volume due to differences in overall head size was taken into account by modelling total intracranial volume as a nuisance covariate. Although the group mean ages were not significantly different, we modelled age as a nuisance covariate, removing age as a potential source of the differences we documented. There is a strong body of evidence linking ageing with an overall reduction in grey matter volume (Pfefferbaum *et al*., 1994; Luft *et al*., 1999; Good *et al*., 2001). However, studies of ageing in visual cortex have demonstrated that there is no observable decrease in neuronal cell count with age (Leuba & Kraftsik, 1994). More recent research has supported this by showing that certain brain regions are less prone to ageing effects, with Raz *et al*. (2004) finding that cortical volume around the calcarine fissure in the occipital lobes remained relatively constant regardless of age. Although we included age as a covariate in the statistical analysis of our data, this may have been overly cautious, given our region of interest centred on the visual cortex.

Having discounted age and head size as possible causes for change in occipital lobe grey matter, the most parsimonious explanation for our observation is that it is directly related to the underdeveloped fovea and reduced ganglion cell numbers in central retina, characteristic of albinism. Whether the structure of afferent visual pathways is affected by these retinal abnormalities has been the subject of previous MRI studies. Whereas Brodsky *et al*. (1993) found no observable differences in size and structure of prechiasmatic optic nerves, optic chiasm and corpus callosum in albinism, a more recent study on a larger subject group found that albinos had a significantly smaller optic chiasm and reduced widths of optic nerves and tracts than controls (Schmitz *et al*., 2003). The latter results are supported by the reduction in the width of the optic nerves, chiasm and tracts in albinism that we demonstrated here. It appears likely that the reduced ganglion cell numbers in central retina observed in the albino primate (Guillery *et al*., 1984) and hypopigmented cat (Stone *et al*., 1978; Leventhal & Creel, 1985), as well as the underdeveloped fovea observed in human albinos (Elschnig, 1913) cause this narrowing in width of optic nerves, chiasm and tracts and therefore further result in the decreased cortical volume at the occipital poles.

The location of the observed reduction in grey matter also supports a direct link with the underdeveloped fovea in albinism. An early study of visual cortex noted that lesions at the posterior ends of the occipital poles were linked with central scotoma (Holmes & Lister, 1916). Since then functional imaging studies have demonstrated retinotopic maps of visual cortex (De Yoe *et al*., 1994; Engel *et al*., 1994, 1997; Sereno *et al*., 1995). Our functional data depict the activation of primary visual cortex in response to stimulation of the central 2° of visual field in a subset of our subjects. This angle of visual arc subtends the fovea and central retina. The resulting cortical activation therefore reflects functional localization of central retina in these subjects. The high degree of overlap between the observed reduction in grey matter in albinism and activated cortex strongly suggests the underdeveloped fovea, characteristic of albinism, is a likely cause of decreased grey matter volume. Furthermore, the retinal abnormalities observed in the albino primate (Guillery *et al*., 1984) were restricted to central retina. Ganglion cell size and density in peripheral retina were similar to its pigmented counterpart. Thus, it appears likely that cortical abnormalities resulting from these retinal deficits would be restricted to the representation of central visual field only.

The small (< 1.6 cm) underlying asymmetry of the VBM cluster centre coordinates is puzzling, but given the relatively large expanse of cortex which is activated by stimulation of the central 2° of visual field and the comparatively small extent of reduced grey matter that was observed, it is possible that the VBM analysis lacks sufficient power to detect adequately the overall extent of grey matter reduction in both hemispheres.

Post-mortem work by Andrews *et al*. (1997) has indicated strong correlations between the sizes of structures in the human visual system, such that a reduction in the size of the optic nerves and tracts is accompanied by a concomitant decrease in size of LGN and V1 visual cortex. Studies in non-human primates have also linked the loss of retinal ganglion cells by enucleation with a reduction in striate cortex (Bourgeois & Rakic, 1996; Dehay *et al*., 1996). Given the decrease in width of optic nerves, chiasm and tracts measured here, and the reduction in central retinal ganglion cell numbers associated with albinism, we would expect a reduction in the size of LGN and V1 in albinism. Our observations denote a significant decrease in grey matter in visual cortex, but the LGN cannot be identified in the T1-weighted images we acquired.

Bodensteiner *et al*. (1990) found a hypoplastic corpus callosum in a case study of a subject with OA, indicating that changes may not be limited to afferent visual pathways. Despite the measured reduction in grey matter volume in visual cortex, we observed no reduction in white matter volume in subjects with albinism, either in the occipital lobes or in the corpus callosum. This may be due to the reduced sensitivity of VBM to changes in white matter (Ashburner & Friston, 2000; Bookstein, 2001). White matter segmentation is also more likely to be confounded by misclassification of white matter and CSF. A larger number of subjects, both control and albino, could sufficiently increase the statistical power such that white matter changes may be detected.

A recent study of subjects with aniridia, who also suffer from foveal hypoplasia, noted a similar reduction in grey matter levels in visual cortex (Free *et al*., 2003). The genetic mutation that gave rise to aniridia in the subjects studied also causes widespread visible cortical abnormalities (Free *et al*., 2003), features that are not present in the

brains of humans with albinism (Brodsky *et al*., 1993). Our study of albinism therefore gives the first demonstration in human of a cortical deficit that results from a retinal deficit in the absence of other widespread cortical abnormalities.

Acknowledgements

This work was supported by the Wellcome Trust (Grant 63343). We would like to thank Donald McRobbie and Rebecca Quest at the Charing Cross Hospital for their assistance.

Abbreviations

CSF, cerebrospinal fluid; FWHM, full-width at half-maximum; MRI, magnetic resonance imaging; OA, ocular albinism; OCA, oculocutaneous albinism; VBM, voxel-based morphometry; VEP, visual evoked potential.

References

Abadi, R.V. & Pascal, E. (1991) Visual resolution limits in human albinism. *Vision Res.*, **31**, 1445–1447.

Akerman, C.J., Tolhurst, D.J., Morgan, J.E., Baker, G.E. & Thompson, I.D. (2003) Relay of visual information to the lateral geniculate nucleus and the visual cortex in albino ferrets. *J. Comp. Neurol.*, **461**, 217–235.

Andrews, T.J., Halpern, S.D. & Purves, D. (1997) Correlated size variations in human visual cortex, lateral geniculate nucleus, and optic tract. *J. Neurosci.*, **17**, 2859–2868.

Ashburner, J. & Friston, K.J. (2000) Voxel-based morphometry – the methods. *Neuroimage*, **11**, 805–821.

Bach, M. (1996) The Freiburg Visual Acuity Test: automatic measurement of visual acuity. *Optom. Vis. Sci.*, **73**, 49–53.

Bodensteiner, J.B., Breen, L., Schwartz, T.L. & Schaeffer, G.B. (1990) Hypoplastic corpus callosum in ocular albinism: indication of a global disturbance of neuronal migration. *J. Child Neurol.*, **5**, 341–343.

Bookstein, F.L. (2001) 'Voxel-based morphometry' should not be used with imperfectly registered images. *Neuroimage*, **14**, 1454–1462.

Bourgeois, J.P. & Rakic, P. (1996) Synaptogenesis in the occipital cortex of macaque monkey devoid of retinal input from early embryonic stages. *Eur. J. Neurosci.*, **8**, 942–950.

Brodsky, M.C., Glasier, C.M. & Creel, D.J. (1993) Magnetic resonance imaging of the visual pathways in human albinos. *J. Pediatr. Ophthalmol. Strabismus*, **30**, 382–385.

Creel, D.J. (1971) Visual system anomaly associated with albinism in the cat. *Nature*, **231**, 465–466.

Creel, D., Witkop, C.J. Jr & King, R.A. (1974) Asymmetric visually evoked potentials in human albinos: evidence for visual system anomalies. *Invest. Ophthalmol.*, **13**, 430–440.

De Yoe, E.A., Bandettini, P., Neitz, J., Miller, D. & Winans, P. (1994) Functional magnetic resonance imaging (FMRI) of the human brain. *J. Neurosci. Meth.*, **54**, 171–187.

Dehay, C., Giroud, P., Berland, M., Killackey, H. & Kennedy, H. (1996) Contribution of thalamic input to the specification of cytoarchitectonic cortical fields in the primate: effects of bilateral enucleation in the fetal monkey on the boundaries, dimensions, and gyrification of striate and extrastriate cortex. *J. Comp. Neurol.*, **367**, 70–89.

Dougherty, R.F., Koch, V.M., Brewer, A.A., Fischer, B., Modersitzki, J. & Wandell, B.A. (2003) Visual field representations and locations of visual areas V1/2/3 in human visual cortex. *J. Vis.*, **3**, 586–598.

Elschnig, A. (1913) Zur Anatomie des menschlichen Albinoauges. *Graefe's Arch. Clin. Exp. Opthalmol.*, **84**, 401–419.

Engel, S.A., Glover, G.H. & Wandell, B.A. (1997) Retinotopic organization in human visual cortex and the spatial precision of functional MRI. *Cereb. Cortex*, **7**, 181–192.

Engel, S.A., Rumelhart, D.E., Wandell, B.A., Lee, A.T., Glover, G.H., Chichilnisky, E.J. & Shadlen, M.N. (1994) fMRI of human visual cortex. *Nature*, **369**, 525.

Free, S.L., Mitchell, T.N., Williamson, K.A., Churchill, A.J., Shorvon, S.D., Moore, A.T., van Heyningen, V. & Sisodiya, S.M. (2003) Quantitative MR image analysis in subjects with defects in the PAX6 gene. *Neuroimage*, **20**, 2281–2290.

Gaser, C. & Schlaug, G. (2003) Brain structures differ between musicians and non-musicians. *J. Neurosci.*, **23**, 9240–9245.

Good, C.D., Johnsrude, I.S., Ashburner, J., Henson, R.N., Friston, K.J. & Frackowiak, R.S. (2001) A voxel-based morphometric study of ageing in 465 normal adult human brains. *Neuroimage*, **14**, 21–36.

Guillery, R.W., Hickey, T.L., Kaas, J.H., Felleman, D.J., Debruyn, E.J. & Sparks, D.L. (1984) Abnormal central visual pathways in the brain of an albino green monkey (*Cercopithecus aethiops*). *J. Comp. Neurol.*, **226**, 165–183.

Guillery, R.W. & Kaas, J.H. (1973) Genetic abnormality of the visual pathways in a 'white' tiger. *Science*, **180**, 1287–1289.

Guillery, R.W., Okoro, A.N. & Witkop, C.J. Jr (1975) Abnormal visual pathways in the brain of a human albino. *Brain Res.*, **96**, 373–377.

Hoffmann, M.B., Tolhurst, D.J., Moore, A.T. & Morland, A.B. (2003) Organization of the visual cortex in human albinism. *J. Neurosci.*, **23**, 8921–8930.

Holmes, G. & Lister, W.T. (1916) Disturbances of vision from cerebral lesions with special reference to the cortical representation of the macula. *Brain*, **39**, 34–73.

Hubel, D.H. & Wiesel, T.N. (1971) Aberrant visual projections in the Siamese cat. *J. Physiol.*, **218**, 33–62.

Jeffery, G., Darling, K. & Whitmore, A. (1994) Melanin and the regulation of mammalian photoreceptor topography. *Eur. J. Neurosci.*, **6**, 657–667.

Kaas, J.H. & Guillery, R.W. (1973) The transfer of abnormal visual field representations from the dorsal lateral geniculate nucleus to the visual cortex in Siamese cats. *Brain Res.*, **59**, 61–95.

Kinnear, P.E., Jay, B. & Witkop, C.J. Jr (1985) Albinism. *Surv. Ophthalmol.*, **30**, 75–101.

Leuba, G. & Kraftsik, R. (1994) Changes in volume, surface estimate, three-dimensional shape and total number of neurons of the human primary visual cortex from midgestation until old age. *Anat. Embryol. (Berl.)*, **190**, 351–366.

Leventhal, A.G. & Creel, D.J. (1985) Retinal projections and functional architecture of cortical areas 17 and 18 in the tyrosinase-negative albino cat. *J. Neurosci.*, **5**, 795–807.

Luft, A.R., Skalej, M., Schulz, J.B., Welte, D., Kolb, R., Burk, K., Klockgether, T. & Voight, K. (1999) Patterns of age-related shrinkage in cerebellum and brainstem observed in vivo using three-dimensional MRI volume try. *Cereb. Cortex*, **9**, 712–721.

Lund, R.D. (1965) Uncrossed visual pathways of hooded and albino rats. *Science*, **149**, 1506–1507.

Maguire, E.A., Gadian, D.G., Johnsrude, I.S., Good, C.D., Ashburner, J., Frackowiak, R.S. & Frith, C.D. (2000) Navigation-related structural change in the hippocampi of taxi drivers. *Proc. Natl Acad. Sci. USA*, **97**, 4398–4403.

Pfefferbaum, A., Mathalon, D.H., Sullivan, E.V., Rawles, J.M., Zipursky, R.B. & Lim, K.O. (1994) A quantitative magnetic resonance imaging study of changes in brain morphology from infancy to late adulthood. *Arch. Neurol.*, **51**, 874–887.

Raz, N., Rodrigue, K.M., Head, D., Kennedy, K.M. & Acker, J.D. (2004) Differential aging of the medial temporal lobe: a study of a five-year change. *Neurology*, **62**, 433–438.

Schmitz, B., Schaefer, T., Krick, C.M., Reith, W., Backens, M. & Kasmann-Kellner, B. (2003) Configuration of the optic chiasm in humans with albinism as revealed by magnetic resonance imaging. *Invest. Ophthalmol. Vis. Sci.*, **44**, 16–21.

Sereno, M.I., Dale, A.M., Reppas, J.B., Kwong, K.K., Belliveau, J.W., Brady, T.J., Rosen, B.R. & Tootell, R.B. (1995) Borders of multiple visual areas in humans revealed by functional magnetic resonance imaging. *Science*, **268**, 889–893.

Stone, J., Rowe, M.H. & Campion, J.E. (1978) Retinal abnormalities in the Siamese cat. *J. Comp. Neurol.*, **180**, 773–782.

Talairach, J. & Tournoux, P. (1988) *Co-Planar Stereotaxic Atlas of the Human Brain*. Thieme, Stuttgart.

Vargha-Khadem, F., Watkins, K.E., Price, C.J., Ashburner, J., Alcock, K.J., Connelly, A., Frackowiak, R.S., Friston, K.J., Pembrey, M.E., Mishkin, M., Gadian, D.G. & Passingham, R.E. (1998) Neural basis of an inherited speech and language disorder. *Proc. Natl Acad. Sci. USA*, **95**, 12695–12700.

Woermann, F.G., Free, S.L., Koepp, M.J., Sisodiya, S.M. & Duncan, J.S. (1999) Abnormal cerebral structure in juvenile myoclonic epilepsy demonstrated with voxel-based analysis of MRI. *Brain*, **122**, 2101–2108.

Worsley, K.J., Marrett, S.N.P., Vandal, A.C., Friston, K.J. & Evans, A.C. (1996) A unified statistical approach for determining significant voxels in images of cerebral activation. *Hum. Brain Mapp.*, **4**, 58–73.

Wright, I.C., McGuire, P.K., Poline, J.B., Travere, J.M., Murray, R.M., Frith, C.D., Frackowiak, R.S. & Friston, K.J. (1995) A voxel-based method for the statistical analysis of gray and white matter density applied to schizophrenia. *Neuroimage*, **2**, 244–252.